

Hierarchical Reinforcement Learning in Complex 3D Environments

Bernardo Avila Pires^{*},¹, Feryal Behbahani^{*},¹, Huber Soyer^{*},¹, Kyriacos Nikiforou^{*},¹, Thomas Keck^{*},¹ and Satinder Singh^{*},¹

^{*}Equal contributions, ¹DeepMind

Hierarchical Reinforcement Learning (HRL) agents have the potential to demonstrate appealing capabilities such as planning and exploration with abstraction, transfer, and skill reuse. Recent successes with HRL across different domains provide evidence that practical, effective HRL agents are possible, even if existing agents do not yet fully realize the potential of HRL. Despite these successes, visually complex partially observable 3D environments remained a challenge for HRL agents. We address this issue with Hierarchical Hybrid Offline-Online (H2O2), a hierarchical deep reinforcement learning agent that discovers and learns to use options from scratch using its own experience. We show that H2O2 is competitive with a strong non-hierarchical Muesli baseline in the DeepMind Hard Eight tasks and we shed new light on the problem of learning hierarchical agents in complex environments. Our empirical study of H2O2 reveals previously unnoticed practical challenges and brings new perspective to the current understanding of hierarchical agents in complex domains.

Keywords: Hierarchical Reinforcement Learning, Partially Observable Markov Decision Processes, Deep Reinforcement Learning

1. Introduction

Hierarchical Reinforcement Learning (HRL; Barto and Mahadevan, 2003; Hutsebaut-Buyse et al., 2022; Pateria et al., 2021; Sutton and Barto, 2018) is a framework that could provide us with general and reusable agent representations and behaviors that can exhibit improved exploration and temporal abstraction (Nachum et al., 2019). The inspiration comes from humans’ ability to break down novel tasks into a sequence of simpler sub-tasks they know how to solve (Solway et al., 2014). This hierarchical approach enables us to transfer our knowledge and reuse our skills to solve new problems.

Contributions. In this work we introduce Hierarchical Hybrid Offline-Online (H2O2), a hierarchical deep reinforcement learning agent that discovers and learns to use options from scratch using its own experience. We show that H2O2 is competitive with a strong non-hierarchical Muesli baseline (Hessel et al., 2021) in the Hard Eight task suite Gulcehre et al. (2019); Ward et al. (2020). These are challenging sparse-reward tasks in a

complex partially observable, first-person 3D environment. H2O2 employs a combination of primitive actions and temporally-extended options selected from a continuous option space¹. To the best of our knowledge, this is the first hierarchical agent that can be competitive with a strong flat baseline in tasks as complex as the Hard Eight suite, while demonstrably using options to solve tasks.

Our work also sheds new light on the problem of learning hierarchical agents and learning options in complex environments. We use H2O2 to test a number of hypotheses about its learning and performance in response to changes in its hierarchical design, and our results reveal previously undetected practical challenges. While some of our experiments support conclusions in line with the conventional understanding of HRL, others challenged our understanding of hierarchical agents. For instance, we observed that seemingly beneficial actions such as increasing the agent’s option space or allowing it to learn

¹We also provide [videos of the agent](#) (see Appendix C.4 for details)

longer options, can actually hurt its performance.

2. Background and Related Work

A common HRL approach is to add options to the MDP, turning it into a semi-MDP (SMDP; Sutton et al., 1999), and then use a general-purpose RL algorithm to solve the SMDP (Barto and Mahadevan, 2003; Dayan and Hinton, 1992). SMDP agents decompose into a low-level controller (LLC, which executes the options in the original MDP) and a high-level controller (HLC, which learns to solve the SMDP). The options may include the actions of the MDP (the *primitive actions*) in addition to temporally extended behaviors *per se*, so that no generality is lost when solving the SMDP instead of solving the MDP “directly”.

The SMDP strategy effectively changes the problem for the general-purpose RL algorithm. It is possible to add various capabilities to the general-purpose RL algorithm by augmenting the SMDP with expressive, diverse options (Barreto et al., 2019), additional/alternative state representations (Dayan and Hinton, 1992; Shah et al., 2022), and even actions to exert fine-grained control over the options (Barto and Mahadevan, 2003; Precup, 2000).

Options can be learned from experience, which can be generated by the hierarchical agent itself (“learned from scratch”; Ajay et al., 2020; Bacon et al., 2017; Eysenbach et al., 2018; Hafner et al., 2022; Harutyunyan et al., 2019; Wulfmeier et al., 2021), or by another agent (for example, an expert; Lynch and Sermanet, 2020; Lynch et al., 2020; Merel et al., 2019). The agent can be learned as one unit (Ajay et al., 2020; Bacon et al., 2017; Merel et al., 2019; Wulfmeier et al., 2021), but one can also decouple the LLC’s option-learning and the HLC’s general-purpose RL algorithm (Dayan and Hinton, 1992; Hafner et al., 2022; Vezhnevets et al., 2017).

There have been recent successes in learning *goal-conditioned* options (Ajay et al., 2020; Khazatsky et al., 2021; Lynch and Sermanet, 2020; Lynch et al., 2020; Machado and Bowling, 2016; Mendonca et al., 2021). These behaviors are trained to produce specific outcomes (observa-

tions or states) in the environment, and they are commonly learned in hindsight from trajectories of agent (Andrychowicz et al., 2017). The idea is to identify goals achieved in each trajectory, and use trajectories as demonstrations of behavior that achieves the goal. The policy can be trained, for example, using behavior cloning (BC; Pomerleau, 1989) or offline RL (Fu et al., 2020; Fujimoto et al., 2019; Gulcehre et al., 2020; Lange et al., 2012; Levine et al., 2020; Nachum et al., 2018). The effectiveness of the learned options is largely affected by the choice of policy-learning algorithm, the data available, and how goals are discovered. For example, BC has been shown to yield effective goal-conditioned policies when used on data generated by experts (Lynch et al., 2020), but not on non-expert data (Ajay et al., 2020), whereas offline RL has shown more promise in the latter case.

Discovering both which sub-behaviors to learn and how to combine them can be tackled by pre-learning skills/behaviors with a variety of signals such as expert demonstrations (Gupta et al., 2020), pseudo-rewards (Barreto et al., 2019), state-space coverage (Eysenbach et al., 2018; Islam et al., 2019; Lee et al., 2019; Pong et al., 2020), empowerment (Gregor et al., 2017), among many others. Alternatively, the agent can learn its sub-behaviors from its own data, that is, “from scratch” (Hafner et al., 2022; Wulfmeier et al., 2021). This approach has the appeal of being end-to-end, and is philosophically aligned with mainstream deep RL, where agents learn on data that is relevant to the task they are expected to perform (Fu et al., 2020; Gulcehre et al., 2020; Mnih et al., 2015; Silver et al., 2018). It is justified on the grounds that a learning agent will ultimately have to collect novel experience and learn novel sub-behaviors on that experience.

The set of options added to the SMDP can also vary. If there are only a few options, they can be learnt as separate entities (Bacon et al., 2017; Wulfmeier et al., 2021). A much larger set of options (and, more specifically, goal conditioned policies), on the other hand, can be learned implicitly by encoding the options (goals) in latent space, and treating any element of the latent space as a valid option (goal) (Ajay et al., 2020;

Hafner et al., 2022; Lynch and Sermanet, 2020; Lynch et al., 2020; Merel et al., 2019). In this case the whole latent space is part of the action space for the SMDP, and the HLC needs to learn to select elements of this latent space. The complexity of the set of options can be, to a certain extent, limited, by regularizing or constraining the latent output of the option encoders (Ajay et al., 2020; Hafner et al., 2022; Lynch and Sermanet, 2020; Lynch et al., 2020; Merel et al., 2019). We are not aware of any successful HRL approaches that encode goals in latent space but do not constrain the latent output of the option encoders in some way. This suggests that some manner of latent space regularization is essential for deep RL SMDP agents, and this hypothesis is consistent with the empirical findings we present in this work. We will see in our experiments that not constraining the latent output of the encoder is detrimental H2O2’s performance.

We are primarily interested in partially observable environments, and we adopt the typical deep RL setup for this type of domain: The agent, at each timestep t , must select the action a_t according to a stochastic policy that can depend on the *history* (the sequence of past observations o_1, \dots, o_t and actions a_1, \dots, a_{t-1}). This reduces the POMDP to an MDP whose states are the histories of past observations and actions (Cassandra et al., 1994). This design choice burdens the deep RL agent with learning to represent histories effectively, but it allows us to use general-purpose deep RL algorithms on both MDPs and POMDPs. For SMDP agents, both the MDP and the SMDP are treated as above: The LLC acts in a partially observable environment reduced to an MDP over histories, and the HLC acts in a partially observable environment reduced to an SMDP over histories.

3. Agent Design

H2O2 is an SMDP agent with options learned from scratch, in offline fashion, that is *decoupled* from the HLC. The options are goal-conditioned: The goals are selected in hindsight from experience and encoded into a latent space; then we use offline RL to train an LLC to attain these goals.

The general-purpose deep RL algorithm used for the HLC is Muesli (Hessel et al., 2021), which has state-of-the-art performance in the Atari benchmark (Bellemare et al., 2013). We train the HLC online, through interaction with the environment, as usual for deep RL agents. Due to our agent’s hierarchical design and how its components are trained, we call it **Hierarchical Hybrid Offline-Online (H2O2)**.

Figure 1 gives an overview of H2O2, and how its components interact with each other and the environment. We outline H2O2’s main compo-

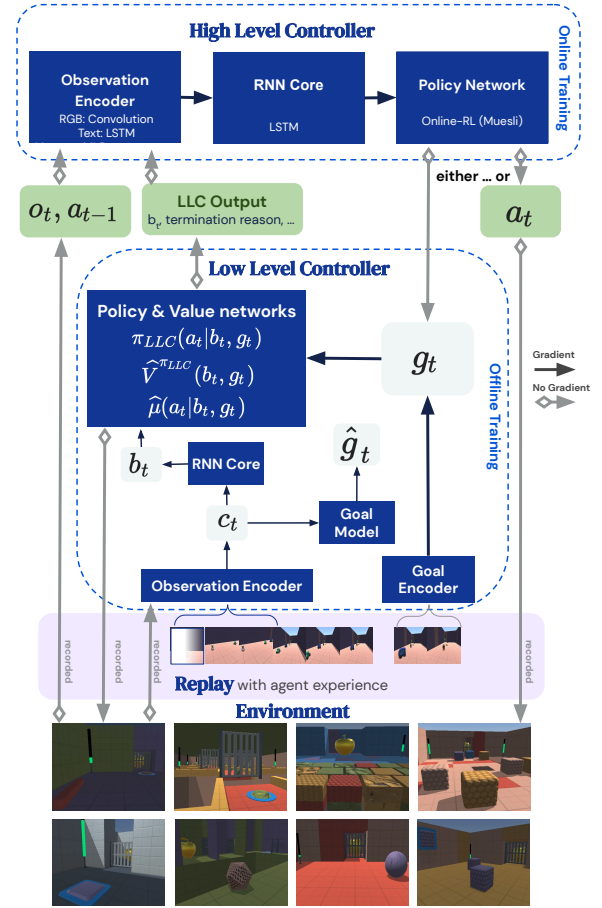


Figure 1 | H2O2 component diagram. The dotted boxes indicate how components (in blue) are trained. The arrows indicate information (inputs, outputs and gradients) passed between components.

ponents in the rest of this section, and we give details in Appendix B.

3.1. Low-Level Controller Design

Training data. The experience generated by H2O2 is inserted into a replay buffer (Cassirer et al., 2021; Horgan et al., 2018) as the agent interacts with the environment. The LLC learner processes minibatches of trajectories sampled (uniformly at random) from the replay (Horgan et al., 2018), where each trajectory has the form $(o_1, a_1, \dots, o_n, a_n)$.

We sample *start* and *end* timesteps t_s, t_e from the set $\{(i, j) : 1 \leq i < j \leq n\}$, encode o_{t_e} with the Goal Encoder (see Fig. 1) to obtain a *latent goal* $g \in [-1, 1]^d$. The sampled goal is fixed for the sampled subtrajectory ($g_{t_s} = g_{t_s+1} = \dots = g_{t_e} = g$) and each subtrajectory is treated as a separate episodic task terminating on timestep t_e (when the goal g is attained). The reward is $r_t \doteq \mathbb{1}\{t = t_e\}$ ($\mathbb{1}$ denotes the indicator function), that is, one for attaining the goal, and zero otherwise. During training we sample multiple pairs t_s, t_e per trajectory in the minibatch, so we train the LLC on multiple tasks (goals) at once.

The LLC’s policy and value function are conditioned on the latent goal g_t and on the agent’s *representation* b_t (the “agent state” Sutton and Barto, 2018). To compute b_t , we process the observations and actions using a recurrent IMPALA-like network (Espeholt et al., 2018) (the Observation Encoder and the RNN Core in Fig. 1). For each t , the representation depends only on the previous observations and actions, and on the recurrent state of the neural network before o_1 .

Goal Sampling during Training. During goal sampling, we reject subtrajectories that are too short or too long (determined by hyperparameters), as well as goals that are too “similar” to other goals (details in Appendix B.1). We also increase the relative frequency of pairs (t_s, t_e) where the reward from the environment is non-zero for some timestep $t_s \leq t \leq t_e$. Increasing the frequency of reward-related goals allowed us to direct the behavior of the LLC to be meaningful for the RL problem, without introducing too much of a dependency on task rewards, rather than learning options that directly optimize for the environment reward (Hafner et al., 2022). Controlling

the goal sampling distribution also provides a direct way to study the option discovery problem using H2O2.

Offline RL. To learn the LLC policy π_{LLC} , we introduce a *regularized* offline V-Trace (Espeholt et al., 2018; Mathieu et al., 2021). π_{LLC} is a distribution over primitive actions that we optimize by following a V-Trace policy gradient. We also regularize π_{LLC} to stay close to an estimate of the behavior policy $\hat{\mu}$, trained with behavior cloning (Pomerleau, 1989). Similar to other offline RL works (Fujimoto et al., 2019; Gulcehre et al., 2021), we found this regularizer to be essential for training an effective LLC, as removing it or annealing it out made the offline RL ineffective.

The gradient step of regularized offline V-Trace is:

$$\frac{\pi_{\text{LLC}}(a_t|b_t, g)}{\hat{\mu}(a_t|b_t, g)} \cdot \text{Adv}_t \cdot \nabla \log \pi_{\text{LLC}}(a_t|b_t, g) - \alpha \nabla \text{KL}(\pi_{\text{LLC}}(b_t, g) | \hat{\mu}(b_t, g)), \quad (1)$$

where Adv_t is the advantage estimate at time t (computed using V-Trace returns and the value estimate $\hat{V}^{\pi_{\text{LLC}}}$, Espeholt et al., 2018), α is a fixed hyperparameter for the KL regularizer, and the gradient is taken only with respect to the parameters of π_{LLC} (without differentiating through $\hat{\mu}$). Differently from the original V-Trace, Eq. (1) uses an estimate of the behavior policy instead of the behavior policy itself.

Following Espeholt et al. (2018), we add a weighted neg-entropy regularizer ($-H(\pi_{\text{LLC}})$) to the objective for π_{LLC} . We train the value function estimate $\hat{V}^{\pi_{\text{LLC}}}$ through regression (as done by Espeholt et al., 2018, and akin to Fitted Q Iteration, Ernst et al., 2005). The representation b_t and the latent goal g_t are shared between π_{LLC} , $\hat{V}^{\pi_{\text{LLC}}}$ and $\hat{\mu}$, and all three learning tasks (regularized policy gradient, value learning and behavior cloning) flow gradients into the representation and the latent goal.

Variational Goal Encoder. Our Goal Encoder is inspired by variational autoencoders (Kingma and Welling, 2013; Rezende et al., 2014) and it outputs a distribution over the goal space from

which we can sample goals g . Concretely, Goal Encoder outputs the parameters of a multivariate normal distribution with diagonal covariance that is used to sample the latent goal g . Differently from VAEs, we do not attempt to autoencode the input of the Goal Encoder from the sampled latent goals, but instead use the sampled latent goals for the Offline RL and auxiliary tasks.

We use a KL regularizer term with weight β to encourage the multivariate normal to stay close to a standard normal distribution. A weight $\beta = 0$ will allow the goal space to be as expressive as afforded by the Goal Encoder, whereas a large enough β will effectively cause the goals g to be sampled from a standard normal distribution (ignoring the observation input to the encoder). The KL regularization is primarily for the benefit of the HLC, as our empirical results will show. We believe that this regularization makes the goal space smoother, and make it easier for the HLC to explore and choose goals.

Auxiliary Tasks. In addition to the learning objectives outlined above, we employed three auxiliary prediction tasks to improve the quality of our LLC.

The first one is training the Goal Model in Fig. 1. via maximum likelihood estimation of latent goals g_t conditioned on c_t (the output of the agent’s Observation Encoder). This is an auxiliary only flow gradients into the observation encoder (not g). We observed that, without this auxiliary task, the LLC would frequently ignore the goal conditioning.

The second auxiliary task is to estimate the state value of the behavior policy, with respect to the environment rewards. The value estimate is a function of b_t and g and flows gradient into both. We found this auxiliary task to be beneficial, and we believe it helps by shaping b_t and g to encode information about rewarding states in the environment.

The third auxiliary task is to predict, from each timestep t , how far in future the goal is. We frame the prediction task as a multiclass logistic classification task. During training, if the goal is on step t_e , then the classification label for each

step t is $t_e - t$, out of n possible classes, where n is an upper-bound on how far into the future goals can be.

3.2. SMDP and High-Level Controller Design

The HLC can instruct the LLC to execute either primitive actions or goals (and the decision of which one to choose at each step is part of the HLC’s policy), and the LLC executes them in the call-and-return model (Dayan and Hinton, 1992).

Option Termination and Initiation. We improved our agent’s sample efficiency by composing simple fixed rules and learned termination/initiation functions. We used a hard limit on option duration (timeout; Sutton et al., 1999) as the fixed rule, and an “attainment classifier” as the learned termination function. We built the attainment classifier from the LLC’s auxiliary task that predicts (via classification) how far in the future the goal is. The option terminates when class 0 (“the goal is attained now”) is the most likely class predicted by the time-to-goal classifier.

The fixed initiation criterion is to allow any goal in any situation (Bacon et al., 2017). However, this is problematic with learned goal-conditioned behavior because it is possible to task the LLC with attaining goals that cannot be attained—either because the goals are implausible, or because the LLC is incapable. When the HLC requests an unattainable goal, the LLC will likely run until timeout, which has a significant cost in environment interactions. We observed this to be very problematic in early training, as the HLC can frequently select unattainable goals, but is oblivious of the sample cost of doing so.

We addressed this issue by terminating options after one step if the goal was unattainable. A goal was deemed unattainable if the value estimate $\widehat{V}^{\pi_{\text{LLC}}}(b_t, g)$ was below a certain threshold. For a high enough threshold, this is a conservative criterion because the value estimates $\widehat{V}^{\pi_{\text{LLC}}}(b_t, g)$ will often only be high for goals that the LLC can achieve.

HLC Observations. The LLC is responsible for what the HLC observes—it may forward environ-

ment observations, and it may also process and combine what has been observed during the execution of an option. In this work, the LLC simply forwards the environment observation to the HLC on the steps where the HLC gets to observe the SMDP and take action.

High-Level Controller. We used Muesli (Hessel et al., 2021) as the general-purpose RL algorithm for the HLC. Muesli is a strong RL agent, and it is among the strongest RL agents in the Atari benchmark (Bellemare et al., 2013). Moreover, it admits policies over continuous and discrete actions, and this allows us to parameterize the policies we need for interacting with the LLC. For additional implementation details see Appendix B.

4. Experiments

4.1. H2O2 is competitive with a strong flat baseline

We evaluated H2O2 in the DeepMind Hard Eight suite (Gulcehre et al., 2019). These tasks are 3D, partially observable, procedurally generated, and they require exploration and complex behavior to solve (see Gulcehre et al. (2019) for detailed task descriptions). The agents are trained in a multi-task setting in all eight tasks. The flat baseline is a Muesli agent, and it has only the minimal, necessary differences from the HLC’s Muesli agent—for example, the action spaces differ between H2O2 and the flat baseline, so the policies need to be changed accordingly. Unless otherwise stated, all quantities reported in this work are binned over number of frames, and averaged across all tasks and over five independent runs. Bands show standard error over independent runs.

Figure 2 shows the average return per episode of H2O2 and the flat baseline as a function of the number of frames generated by interacting with the environment (i.e., *throughout training*). The plot shows that the two agents are competitive, with H2O2 attaining slightly higher performance more frequently. We report per-task performance in Fig. 9 in Appendix C.1, where we can see different variations of sample efficiency and final performance between the two agents across tasks.

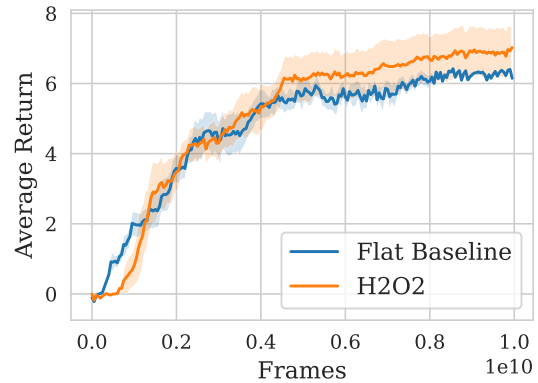


Figure 2 | Average episode return for H2O2 and the Muesli baseline.

H2O2’s improved performance is a demonstration of the effectiveness of our hierarchical agent, but the variations between H2O2 and the flat baseline performances in each task suggest that H2O2 is indeed learning differently from the flat baseline. How is the hierarchical design influencing H2O2’s learning and final performance? What HRL capabilities is H2O2 demonstrating?

4.2. Is H2O2 using temporally extended behaviors?

Yes, but we did not observe that “the more temporal extension, the better”. We found that parameters that control temporal extension have to be carefully selected in order to obtain better performance and even, “paradoxically”, temporally extended behavior. The apparent paradox stems from considering the benefits of increasing temporal extension, without accounting for how it impacts the learning problem. That is, an effective hierarchical agent with more temporally extended behavior is expected to perform at least as well as one with less temporally extended behavior, but giving an untrained agent access to more temporally extended behavior may make the learning problem harder. The problem may be so hard that even after significant training the learning agent may have subpar performance and it may fail to display any meaningful hierarchical behavior.

To substantiate our claim, we measured the average number of environment (LLC) steps per

SMDP (HLC) step, as well as task performance, of different variants of H2O2. Higher values of “average LLC steps” (per HLC step) mean H2O2 spent more timesteps in temporally extended behavior. An agent that exclusively executed primitive actions would have a ratio of 1. This ratio allows us to infer the fraction of steps spent executing options excluding the first step, which for the purpose of our discussion is how much temporally extended behavior an agent displays.

The typical range for the the average LLC steps is between 1.0 and 2.5. An average LLC steps ratio of 1.5 means the agent is in temporally extended behavior for about $\frac{1}{3}$ of its interaction with the base environment. A ratio of 1.25 corresponds to temporal extension in at least 20% of the interaction, and a ratio of 2.5 is corresponds to at least 60%.

H2O2 with different option timeouts. We considered variants of H2O2 with different timeouts: 7, 16 and 32 steps (the timeout used for H2O2 in Fig. 2 was 7). Options terminate when either the goal is attained (according to the LLC’s classifier) or at timeout. Because the options have a termination function, we would expect that increasing timeout should increase the effectiveness and frequency of the agent’s temporally extended behavior. Figure 3a shows, however, that this is not the case. Surprisingly, attempting to increase

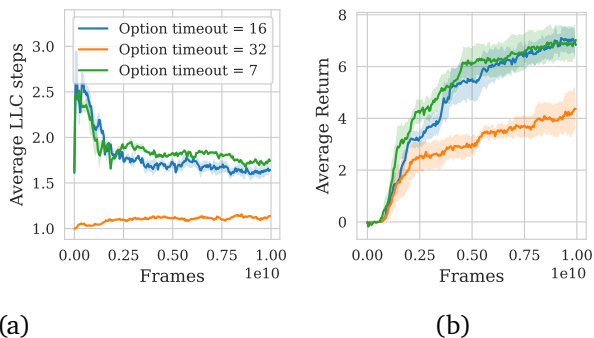


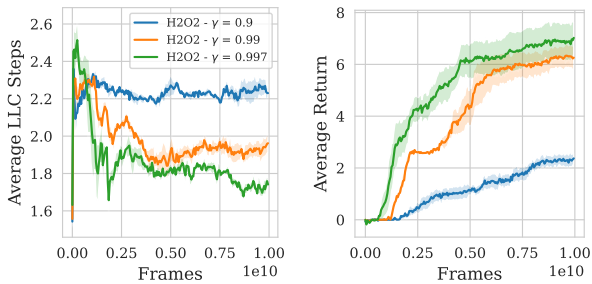
Figure 3 | Evaluation of H2O2 with different option timeouts. (a) Average number of LLC steps per HLC steps throughout training All curves are at approximately 1.0 in the initial training steps; the apparent start of some curves at higher values is an artifact of binning. (b) Average return of H2O2 for different option timeouts.

the amount of temporal abstraction by increasing timeouts eventually *harms* H2O2’s ability to employ temporally extended behavior. Moreover, H2O2’s performance is surprisingly sensitive to the amount of temporal abstraction: even with a timeout of 16 (which has roughly the same amount of temporally extended behavior (Fig. 3a) as the timeout of 7), H2O2’s performance is worse than with a timeout of 7 (see Fig. 3b). The performance with the timeout of 32 is worst, so this setting leads to poor behavior both in terms of temporal abstraction and task performance.

Our data suggests that H2O2 with a timeout of 32 breaks down because the learning problem is too hard. We measured why and how often options terminate throughout training (see Fig. 10), and we saw that in this setting our agent spends about half of the first $2 \cdot 10^9$ frames issuing invalid goals (and thus generating transitions with no-ops). So we suspect that the HLC failed to generate “good” data for the LLC to learn effective goal-following behavior, which in turn led to an unnecessarily challenging SMDP for the HLC to solve, that is, one filled with useless options that waste several frames of environment interaction.

H2O2 with different discounts. We also considered three variants of H2O2 with different discounts γ , in $\{0.9, 0.99, 0.997\}$ (the value used for H2O2 in Fig. 2 was 0.997). Since the discounting only incides on HLC timesteps, the rewards n timesteps in the future will only be discounted by γ^n , even if the amount of primitive actions required to get to that state is significantly larger. For example, if options take an average of 1.5 steps, $\gamma = 0.9$ and $n = 10$, the reward for HLC would be discounted with 0.59, whereas a flat agent executing the same actions would see the reward discounted with 0.21. This “horizon shortening” is expected to encourage the agent to use options, so we expect to see the variants with smaller γ using more options. Figure 4a shows that this is indeed the case.

Figure 4b shows that as we decrease γ the agent spends more time in temporally extended behavior. HRL folklore suggests that the agent with more temporally extended behavior will perform better, because it will be able to assign credit at



(a) Average number of LLC steps per option. (b) Average return.

Figure 4 | Option use (left) and performance (right) for H2O2 with different discount factors γ .

longer timescales. The results in Fig. 4b are evidence against this claim: The plot shows that H2O2 with the largest γ performs best, and that decreasing γ worsens performance (even though it increases option use, as shown in Fig. 4a). The issue is that changing γ also affects the objective of the HLC, and that changing the objective can change both the final solution and how the agent explores. Our hypothesis is that H2O2 with lower γ explores worse, possibly in three ways: 1) The HLC fails to generate behavior with higher rewards because it is optimizing for short-term cumulative reward; 2) The options learned from the poor-performing HLC are also poor (with respect to the task), and the agent is incentivized to choose poor-performing options over exploring further with primitive actions; 3) The longer options also reduce the amount of training data the HLC generates for itself; that is, the HLC is incentivized to generate less data for itself by using options. This third point makes the agent sample inefficient!

Appendix C.3 shows that H2O2 outperforms a simpler idea of adding temporal abstraction to a flat baseline by increasing the number of repeated actions.

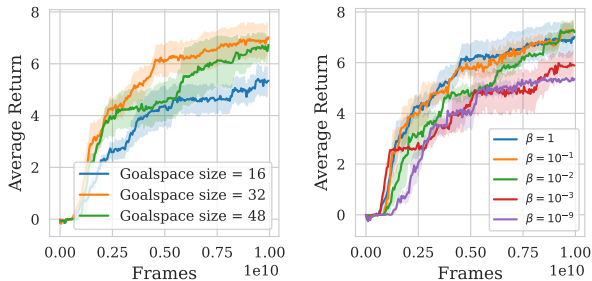
4.3. Does H2O2 benefit from more options?

Sometimes, and we argue that it depends on whether the options *simplify the problem*.

HRL folklore suggests that making more skills available to the HLC empowers the agent and

leads to better solutions. We claim that this is not necessarily the case, and that in H2O2, for learned options to be beneficial, they must *simplify* the problem for the HLC. That is, it does not make sense to solve an SMDP that is harder to solve than the original MDP—in that case we are better off using the flat agent. We considered two ways to offer more options to H2O2: Increasing the dimension of the latent goals, and reducing the amount of regularization on the goal space.

Figure 5a shows the performance of H2O2 where we varied the dimension of the latent goals. We considered dimensions in $\{16, 32, 48\}$, and H2O2 from Fig. 2 uses 32. We see in the figure



(a) Average return for H2O2 with different latent goal dimensions. (b) Average return for H2O2 with different amounts of goal compression. The higher β , the more compression there is.

Figure 5 | Effect of constraining the space of options on overall performance.

that this dimension behaves like a usual hyperparameter: There’s a sweetspot for highest performance at 32, but going lower or higher leads to worse performance. It is surprising, though, that a dimension of 32 works best, as we were initially expecting more expressive goals to be more effective.

We also evaluated the effect the Goal Encoder regularizer on the performance of H2O2. We considered $\beta \in \{10^{-9}, 10^{-3}, 10^{-2}, 10^{-1}, 1\}$. When $\beta = 10^{-9}$ there is no compression of the goal space, but when $\beta = 1$ the regularization is so strong that the posterior is also a standard normal. We used $\beta = 1$ for H2O2 in Fig. 2.

Figure 5b shows the performance of H2O2 for the different values of β , and we see that H2O2

with the least diverse set of options ($\beta = 1$) performs best, along with the larger values of β . The data is consistent with the hypothesis that too much flexibility in the goal space makes the learning problem harder, so adding more options eventually damages the performance of the agent.

4.4. How does H2O2 perform in similar domains from related work?

The work of [Hafner et al. \(2022\)](#) is the closest to ours: They introduced Director, a hierarchical deep RL agent for complex partially observable, first-person 3D environments. It was evaluated in `Goals Small` and `Objects Small` in the DeepMind Lab environment ([Beattie et al., 2016](#)). These are first-person maze tasks that require navigation, localization and recalling reward locations within an episode. Director is an SMDP agent with call-and-return options, but without access to primitive actions, and all options terminate after a fixed number of steps. The options are “state”-directed, in the sense that the LLC (“Worker”) is conditioned on latent vectors from the latent state space (the analogue of our b_t in Fig. 1), and is trained in hindsight for achieving the corresponding latent states. [Hafner et al. \(2022\)](#) use a VQ-VAE ([Razavi et al., 2019](#); [Van Den Oord et al., 2017](#)) to discretize the latent state space, which gives the HLC (“Manager”) a discrete action space. Moreover, they use a World Model ([Hafner et al., 2019b](#)) to help shape Director’s state representation. During training, the LLC in Director is rewarded proportionally to the similarity of its latent state and the conditioning input (the goal), at each timestep. The version of Director that is competitive with their baseline (Dreamer; [Hafner et al., 2019a](#)) adds extrinsic rewards to the reward provided to the LLC.

We evaluated H2O2 and our flat Muesli baseline in DeepMind Lab’s `Goals Small` and `Objects Small`. Figure 6 shows the average return of different agents on the two tasks. The “Flat Baseline” is a Muesli agent like the one used in the Hard Eight tasks, but uses a replay-to-online ratio of 0.9² We present variants of

²This ratio means that in each minibatch 90% of the data is sampled from a replay, and the other 10% from online experience. This increases the data efficiency of the

H2O2 with the replay-to-online ratio used for Hard Eight tasks (0.5) as well as 0.9. The figure also shows the final performance of Director and Dreamer (as the dotted line, both methods have the same final performance). This variant of Director adds extrinsic rewards to the LLC objective. Figure 6 shows that with an appropriate

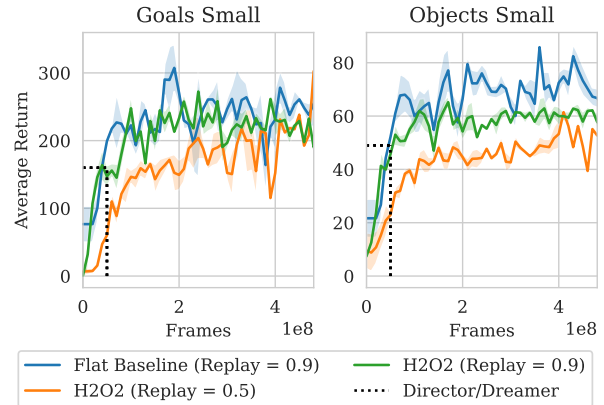


Figure 6 | The average return across two levels of DMLab [Beattie et al. \(2016\)](#). We also indicate the final performance of the Dreamer and Director baselines [Hafner et al. \(2022\)](#) with the dotted line, after 50M frames.

replay-to-online ratio both H2O2 and Muesli baseline can match the data efficiency of Director and Dreamer, though it’s unclear what the latter’s final performance would be if trained longer.

5. Conclusion

Our work introduces H2O2, the first demonstration of a complete hierarchical agent that can use non-trivial options to attain strong performance in visually complex partially observable tasks. H2O2 is competitive with a state-of-the-art flat baseline, it discovers and learns to use its options, and it does so from its own generated experience.

Relevance. HRL has received much interest due to its potential to deliver powerful agents with appealing capabilities—for example, transfer, skill reuse, planning and exploration with abstraction. Recent successes with HRL in different domains

agents and make them competitive in early training (the 180-thousand-frame regime).

(Hafner et al., 2022; Merel et al., 2019; Wulfmeier et al., 2021) provide evidence that practical, effective HRL agents are possible, even if existing agents do not yet fully realize the potential of HRL. Therefore, it is important to expand the coverage of effective hierarchical agents across domains, and to identify and tackle practical challenges that can bring us closer to a full-fledged hierarchical agent.

Significance. Our work is an important contribution to the HRL research for two reasons: H2O2 is a proof of concept, complete and effective HRL agent, and our work highlights critical challenges for HRL in complex domains that are vastly overlooked in the literature. It was only by going through the process of designing and training a HRL agent for complex domains that we exposed some of these issues.

Successes. We built on existing work to tackle some of the practical challenges of HRL in complex domains, such as learning goal-conditioned behaviors offline from any experience generated by an agent (not just expert behavior). To achieve this, we introduced a regularized offline V-Trace algorithm and demonstrated how to integrate the policy that executes these goal-conditioned behaviors (the LLC) with a general-purpose RL algorithm that learns to select these behaviors as options in order to solve tasks (the HLC).

Lessons learned. We believe that our empirical findings apply to domains where a very large number of options is conceivable, but for any one task a much smaller set of behaviors is relevant and useful. Visually complex domains tend to naturally have this property, and this is arguably the kind of rich domain we want intelligent agents to be effective in. However, we think that many of the challenges we observed would go away if we were to limit the learning to a small set of options (Merel et al., 2019; Wulfmeier et al., 2021), or choose them sensibly beforehand.

Within the scope of these “rich domains”, however, the lessons we can draw from our experimental results can apply to various HRL agents beyond H2O2. The lessons apply most closely to

SMDP agents. The SMDP framework has been backed with theoretical justification (Barto and Mahadevan, 2003; Precup, 2000), and our work complements existing knowledge with empirical findings.

We noticed a strong contrast between how HRL is typically motivated in the literature (e.g., Barto and Mahadevan, 2003; Hutsebaut-Buysse et al., 2022; Pateria et al., 2021), and the practical challenges we encountered. It is often claimed that hierarchical agents can demonstrate very appealing capabilities and algorithmic strengths, such as sample efficiency, structured exploration, temporal abstraction, improved credit assignment, state abstraction, jumpy planning, transfer and generalization. These “HRL promises” can easily be misconstrued as properties of hierarchical agents, which may lead to misconceptions about how hierarchical agents will learn and perform.

Our empirical findings exposed some of these HRL misconceptions. For example, the SMDP approach promises to simplify the problem for the general-purpose RL algorithm. So one might expect that adding capabilities that are perceived as strengths of HRL (for example, more expressive options) to the SMDP will cause the general-purpose RL algorithm to solve the SMDP with less effort than if it had simpler options, or only primitive actions. However, in some experiments we showed the opposite.

In practice, the design of the LLC effectively changes the SMDP, and the hierarchical agent can only be competitive with a flat agent if SMDP is easier to solve than the original MDP (besides admitting a better solution). Therefore both solution quality and learning dynamics are essential factors to consider when designing the hierarchical agent.

Open challenges. We also identified questions that remain open: How can we structure the goal space to accelerate the HLC learning? Is it possible to learn effective HLCs with a general-purpose RL algorithms? How can the HLC agent learn with a very large number of complex options, but remain competitive with a flat baseline? Are image goals good enough? What other goal modalities can we use? Which goals should we train the

LLC to achieve?

Some of these questions can be investigated in simple domains, as long as the domains are designed to pose challenges that we observe in practice. For example, a simple grid-world where there is an option to reach any cell from any other cell can be a fruitful domain to explore. However, it may be challenging to outperform strong flat deep RL baselines in such simple domains if the options are not prescribed but learned end to end.

We presented simple approaches for some of the challenges above—e.g. the goal sampling distribution for the LLC. We expect that the performance of H2O2 will improve with goal sampling distributions that incorporate principled techniques for option discovery (Machado and Bowling, 2016). H2O2 can be a starting point for research that aims to investigate specific HRL sub-problems without losing sight of the performance of the whole agent in complex tasks.

References

- A. Ajay, A. Kumar, P. Agrawal, S. Levine, and O. Nachum. Opal: Offline primitive discovery for accelerating offline reinforcement learning. *arXiv preprint arXiv:2010.13611*, 2020.
- M. Andrychowicz, F. Wolski, A. Ray, J. Schneider, R. Fong, P. Welinder, B. McGrew, J. Tobin, O. Pieter Abbeel, and W. Zaremba. Hindsight experience replay. In I. Guyon, U. V. Luxburg, S. Bengio, H. Wallach, R. Fergus, S. Vishwanathan, and R. Garnett, editors, *Advances in Neural Information Processing Systems*, volume 30. Curran Associates, Inc., 2017.
- P.-L. Bacon, J. Harb, and D. Precup. The option-critic architecture. In *Proceedings of the AAAI Conference on Artificial Intelligence*, volume 31, 2017.
- A. Barreto, D. Borsa, S. Hou, G. Comanici, E. Aygün, P. Hamel, D. Toyama, J. Hunt, S. Mourad, D. Silver, and D. Precup. The option keyboard combining skills in reinforcement learning. In *Proceedings of the 33rd International Conference on Neural Information Processing Systems*, pages 13052–13062, 2019.
- A. G. Barto and S. Mahadevan. Recent advances in hierarchical reinforcement learning. *Discrete event dynamic systems*, 13(1):41–77, 2003.
- C. Beattie, J. Z. Leibo, D. Teplyashin, T. Ward, M. Wainwright, H. Küttler, A. Lefrancq, S. Green, V. Valdés, A. Sadik, J. Schrittwieser, K. Andeson, S. York, M. Cant, A. Cain, A. Bolton, S. Gaffney, H. King, D. Hassabis, S. Legg, and S. Petersen. Deepmind lab. *arXiv preprint arXiv:1612.03801*, 2016.
- M. G. Bellemare, Y. Naddaf, J. Veness, and M. Bowling. The arcade learning environment: An evaluation platform for general agents. *Journal of Artificial Intelligence Research*, 47:253–279, 2013.
- A. R. Cassandra, L. P. Kaelbling, and M. L. Littman. Acting optimally in partially observable stochastic domains. In *Aaai*, volume 94, pages 1023–1028, 1994.
- A. Cassirer, G. Barth-Maron, E. Brevdo, S. Ramos, T. Boyd, T. Sottiaux, and M. Kroiss. Reverb: A framework for experience replay, 2021.
- P. Dayan and G. E. Hinton. Feudal reinforcement learning. *Advances in neural information processing systems*, 5, 1992.
- D. Ernst, P. Geurts, and L. Wehenkel. Tree-based batch mode reinforcement learning. *Journal of Machine Learning Research*, 6:503–556, 2005.
- L. Espeholt, H. Soyer, R. Munos, K. Simonyan, V. Mnih, T. Ward, Y. Doron, V. Firoiu, T. Harley, I. Dunning, S. Legg, and K. Kavukcuoglu. Impala: Scalable distributed deep-rl with importance weighted actor-learner architectures. In *International Conference on Machine Learning*, pages 1407–1416. PMLR, 2018.
- B. Eysenbach, A. Gupta, J. Ibarz, and S. Levine. Diversity is all you need: Learning skills without a reward function. In *International Conference on Learning Representations*, 2018.
- J. Fu, A. Kumar, O. Nachum, G. Tucker, and S. Levine. D4rl: Datasets for deep data-driven reinforcement learning. *arXiv preprint arXiv:2004.07219*, 2020.
- S. Fujimoto, D. Meger, and D. Precup. Off-policy deep reinforcement learning without exploration. In K. Chaudhuri and R. Salakhutdinov, editors,

- Proceedings of the 36th International Conference on Machine Learning*, volume 97 of *Proceedings of Machine Learning Research*, pages 2052–2062. PMLR, 09–15 Jun 2019.
- K. Gregor, D. J. Rezende, and D. Wierstra. Variational intrinsic control. In *International Conference on Learning Representations*, 2017.
- C. Gulcehre, T. Le Paine, B. Shahriari, M. Denil, M. Hoffman, H. Soyer, R. Tanburn, S. Kapurkowski, N. Rabinowitz, D. Williams, G. Barth-Maron, Z. Wang, N. de Freitas, and Worlds Team. Making efficient use of demonstrations to solve hard exploration problems. In *International conference on learning representations*, 2019.
- C. Gulcehre, Z. Wang, A. Novikov, T. Paine, S. Gómez, K. Zolna, R. Agarwal, J. S. Merel, D. J. Mankowitz, C. Paduraru, G. Dulac-Arnold, J. Li, M. Norouzi, M. Hoffman, N. Heess, and N. de Freitas. Rl unplugged: A suite of benchmarks for offline reinforcement learning. In H. Larochelle, M. Ranzato, R. Hadsell, M. F. Balcan, and H. Lin, editors, *Advances in Neural Information Processing Systems*, volume 33, pages 7248–7259. Curran Associates, Inc., 2020.
- C. Gulcehre, S. G. Colmenarejo, Z. Wang, J. Synchronowski, T. Paine, K. Zolna, Y. Chen, M. Hoffman, R. Pascanu, and N. de Freitas. Regularized behavior value estimation. *arXiv preprint arXiv:2103.09575*, 2021.
- A. Gupta, V. Kumar, C. Lynch, S. Levine, and K. Hausman. Relay policy learning: Solving long-horizon tasks via imitation and reinforcement learning. In *Conference on Robot Learning*, pages 1025–1037. PMLR, 2020.
- D. Hafner, T. Lillicrap, J. Ba, and M. Norouzi. Dream to control: Learning behaviors by latent imagination. *arXiv preprint arXiv:1912.01603*, 2019a.
- D. Hafner, T. Lillicrap, I. Fischer, R. Villegas, D. Ha, H. Lee, and J. Davidson. Learning latent dynamics for planning from pixels. In *International conference on machine learning*, pages 2555–2565. PMLR, 2019b.
- D. Hafner, K.-H. Lee, I. Fischer, and P. Abbeel. Deep hierarchical planning from pixels. *arXiv preprint arXiv:2206.04114*, 2022.
- A. Harutyunyan, W. Dabney, D. Borsa, N. Heess, R. Munos, and D. Precup. The termination critic. *arXiv preprint arXiv:1902.09996*, 2019.
- M. Hessel, H. Soyer, L. Espeholt, W. Czarnecki, S. Schmitt, and H. van Hasselt. Multi-task deep reinforcement learning with popart. In *Proceedings of the AAAI Conference on Artificial Intelligence*, volume 33, pages 3796–3803, 2019.
- M. Hessel, I. Danihelka, F. Viola, A. Guez, S. Schmitt, L. Sifre, T. Weber, D. Silver, and H. van Hasselt. Muesli: Combining improvements in policy optimization. *arXiv preprint arXiv:2104.06159*, 2021.
- D. Horgan, J. Quan, D. Budden, G. Barth-Maron, M. Hessel, H. van Hasselt, and D. Silver. Distributed prioritized experience replay. In *International Conference on Learning Representations*, 2018.
- M. Hutsebaut-Buysse, K. Mets, and S. Latré. Hierarchical reinforcement learning: A survey and open research challenges. *Machine Learning and Knowledge Extraction*, 4(1):172–221, 2022.
- R. Islam, Z. Ahmed, and D. Precup. Marginalized state distribution entropy regularization in policy optimization. *arXiv preprint arXiv:1912.05128*, 2019.
- A. Khazatsky, A. Nair, D. Jing, and S. Levine. What can i do here? learning new skills by imagining visual affordances. In *2021 IEEE International Conference on Robotics and Automation (ICRA)*, pages 14291–14297. IEEE, 2021.
- D. P. Kingma and M. Welling. Auto-encoding variational bayes. *arXiv preprint arXiv:1312.6114*, 2013.
- S. Lange, T. Gabel, and M. Riedmiller. Batch reinforcement learning. In *Reinforcement learning*, pages 45–73. Springer, 2012.
- L. Lee, B. Eysenbach, E. Parisotto, E. Xing, S. Levine, and R. Salakhutdinov. Efficient exploration via state marginal matching. *arXiv preprint arXiv:1906.05274*, 2019.
- S. Levine, A. Kumar, G. Tucker, and J. Fu. Offline reinforcement learning: Tutorial, review, and perspectives on open problems. *arXiv preprint arXiv:2005.01643*, 2020.

- C. Lynch and P. Sermanet. Grounding language in play. *arXiv preprint arXiv:2005.07648*, 2020.
- C. Lynch, M. Khansari, T. Xiao, V. Kumar, J. Tompson, S. Levine, and P. Sermanet. Learning latent plans from play. In *Conference on Robot Learning*, pages 1113–1132. PMLR, 2020.
- M. C. Machado and M. Bowling. Learning purposeful behaviour in the absence of rewards. *arXiv preprint arXiv:1605.07700*, 2016.
- M. Mathieu, S. Ozair, S. Srinivasan, C. Gulcehre, S. Zhang, R. Jiang, T. Le Paine, K. Zolna, R. Powell, J. Schrittwieser, D. Choi, P. Georgiev, D. Toyama, A. Huang, R. Ring, I. Babuschkin, T. Ewalds, M. Bordbar, S. Henderson, S. G. Colmenarejo, W. M. van den Oord, Aäron Czarnecki, N. de Freitas, and O. Vinyals. Starcraft ii unplugged: Large scale offline reinforcement learning. In *Deep RL Workshop NeurIPS 2021*, 2021.
- R. Mendonca, O. Rybkin, K. Daniilidis, D. Hafner, and D. Pathak. Discovering and achieving goals via world models. *Advances in Neural Information Processing Systems*, 34:24379–24391, 2021.
- J. Merel, L. Hasenclever, A. Galashov, A. Ahuja, V. Pham, G. Wayne, Y. W. Teh, and N. Heess. Neural probabilistic motor primitives for humanoid control. In *International Conference on Learning Representations*, 2019.
- V. Mnih, K. Kavukcuoglu, D. Silver, A. A. Rusu, J. Veness, M. G. Bellemare, A. Graves, M. Riedmiller, A. K. Fidjeland, G. Ostrovski, S. Petersen, C. Beattie, A. Sadik, I. Antonoglou, H. King, D. Kumaran, D. Wierstra, S. Legg, and D. Hassabis. Human-level control through deep reinforcement learning. *nature*, 518(7540):529–533, 2015.
- O. Nachum, S. S. Gu, H. Lee, and S. Levine. Data-efficient hierarchical reinforcement learning. *Advances in Neural Information Processing Systems*, 31:3303–3313, 2018.
- O. Nachum, H. Tang, X. Lu, S. Gu, H. Lee, and S. Levine. Why does hierarchy (sometimes) work so well in reinforcement learning? *arXiv preprint arXiv:1909.10618*, 2019.
- S. Pateria, B. Subagdja, A.-h. Tan, and C. Quek. Hierarchical reinforcement learning: A comprehensive survey. *ACM Computing Surveys (CSUR)*, 54(5):1–35, 2021.
- D. A. Pomerleau. Alvin: An autonomous land vehicle in a neural network. In D. Touretzky, editor, *Advances in Neural Information Processing Systems*, volume 1. Morgan-Kaufmann, 1989.
- V. Pong, M. Dalal, S. Lin, A. Nair, S. Bahl, and S. Levine. Skew-fit: State-covering self-supervised reinforcement learning. In *International Conference on Machine Learning*, pages 7783–7792. PMLR, 2020.
- D. Precup. *Temporal abstraction in reinforcement learning*. University of Massachusetts Amherst, 2000.
- A. Razavi, A. Van den Oord, and O. Vinyals. Generating diverse high-fidelity images with vq-vae-2. *Advances in neural information processing systems*, 32, 2019.
- D. J. Rezende, S. Mohamed, and D. Wierstra. Stochastic backpropagation and approximate inference in deep generative models. In *International conference on machine learning*, pages 1278–1286. PMLR, 2014.
- D. Shah, P. Xu, Y. Lu, T. Xiao, A. Toshev, S. Levine, and B. Ichter. Value function spaces: Skill-centric state abstractions for long-horizon reasoning. In *International Conference on Learning Representations*, 2022.
- D. Silver, T. Hubert, J. Schrittwieser, I. Antonoglou, M. Lai, A. Guez, M. Lanctot, L. Sifre, D. Kumaran, T. Graepel, T. Lillicrap, K. Simonyan, and D. Hassabis. A general reinforcement learning algorithm that masters chess, shogi, and go through self-play. *Science*, 362(6419):1140–1144, 2018.
- A. Solway, C. Diuk, N. Córdova, D. Yee, A. G. Barto, Y. Niv, and M. M. Botvinick. Optimal behavioral hierarchy. *PLoS computational biology*, 10(8):e1003779, 2014.
- R. S. Sutton and A. G. Barto. *Reinforcement Learning: An Introduction*. A Bradford Book, Cambridge, MA, USA, 2018. ISBN 0262039249.
- R. S. Sutton, D. Precup, and S. Singh. Between mdps and semi-mdps: A framework for temporal abstraction in reinforcement learning. *Artificial intelligence*, 112(1-2):181–211, 1999.
- A. Van Den Oord, O. Vinyals, and K. Kavukcuoglu. Neural discrete representation learning. *Ad-*

vances in neural information processing systems, 30, 2017.

A. S. Veohnevets, S. Osindero, T. Schaul, N. Heess, M. Jaderberg, D. Silver, and K. Kavukcuoglu. Feudal networks for hierarchical reinforcement learning. In *International Conference on Machine Learning*, pages 3540–3549. PMLR, 2017.

T. Ward, A. Bolt, N. Hemmings, S. Carter, M. Sanchez, R. Barreira, S. Noury, K. Anderson, J. Lemmon, J. Coe, P. Trochim, T. Handley, and A. Bolton. Using Unity to help solve intelligence, 2020.

M. Wulfmeier, D. Rao, R. Hafner, T. Lampe, A. Abdolmaleki, T. Hertweck, M. Neunert, D. Tirumala, N. Siegel, N. Heess, and M. Riedmiller. Data-efficient hindsight off-policy option learning. In *International Conference on Machine Learning*, pages 11340–11350. PMLR, 2021.

A. SMDP Agent Design Details

An RL agent interacts with a semi-MDP (SMDP; Sutton et al., 1999) by selecting options (temporally extended behaviors with initiation and termination conditions), whereas an RL agent interacting with an MDP (Sutton and Barto, 2018) selects (primitive) actions. Figure 7 outlines these interaction loops, which are intentionally similar. We can turn an MDP into an SMDP by adding

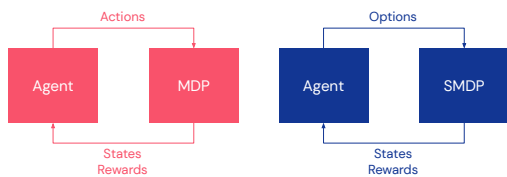


Figure 7 | Agent-environment interaction diagrams for MDPs (left) and SMDPs (right).

options to it. When we learn the options with RL, it is useful to structure the agent interaction in terms of a high-level controller (HLC) which interacts with the SMDP, and a low-level controller (LLC), which interacts with the MDP and provides the options for the SMDP. Figure 8 outlines the interaction loops for the LLC and the HLC. The diagram corresponds to how we structured the HLC and LLC in H2O2.

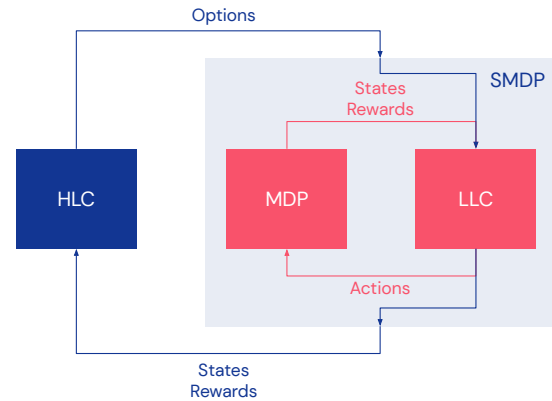


Figure 8 | Agent-environment interaction diagrams for an SMDP, framed in terms of high-level and low-level controllers.

The LLC interacts directly with the MDP (the agent-MDP interaction in the left diagram of Fig. 8, in red). It is responsible for changing its behavior in response to the options received, and for providing the SMDP states and rewards for the HLC, based on the MDP states and rewards it observes.

The LLC executes options in the call-and-return model (Dayan and Hinton, 1992): The HLC selects an option, then the LLC executes the option until it terminates, then returns control to the HLC. From the perspective of the HLC, the interaction with the environment is an agent-SMDP interaction (the right diagram in Fig. 8, in dark blue).

In our work, the LLC allows the HLC to select primitive actions (Sutton et al., 1999), which are implemented as one-step options where the LLC executes the action requested by the HLC. Our LLC forwards environment observations to the HLC along with a “termination reason”. The termination reason is a flag indicating why the LLC execution terminated, and it can be one of the following:

- First timestep: The first timestep in an MDP episode requires the HLC to select an action in the SMDP for the LLC to perform.
- Last timestep: The last timestep in an MDP episode is also the last timestep in the corresponding SMDP.
- The option terminated. In this case the ter-

mination reason encodes why the option terminated. This could be because the goal was attained, the option timed out, or because it was a primitive action (which is framed as a one-step option).

- The option failed to initiate. This is because the goal corresponding to the option is deemed unattainable. The LLC executes a no-op in the environment and terminates. The forced no-op is an implementation decision to prevent the HLC from selecting unattainable goals indefinitely.

B. Implementation details

B.1. Goal Sampling Distribution

We rejected “similar” goals as follows: In a trajectory of potential goals g_1, \dots, g_n , we first identify, for each candidate goal g_t , the closest that any other goal is:

$$\text{sim}_t \doteq \max_{t'} \frac{\langle g_t, g_{t'} \rangle}{\|g_t\|_2 \|g_{t'}\|_2}.$$

Then we exclude all pairs (t_s, t_e) from sampling, such that sim_{t_e} is larger than the 40-percentile of $(\text{sim}_1, \dots, \text{sim}_n)$.

B.2. Low-Level Controller

Image Observations and Goals. Image observations and image goals were 72×96 RGB first-person views of the environment, encoded with a ResNet followed by an MLP (Hessel et al., 2019). For detailed information on the various model hyper-parameters, refer to Table 1.

Vector Goals and Goal Distributions for the affordance model. Throughout this work, we used a goal space defined as $\mathcal{G} = [-1, 1]^{32}$. We explained how the this goal space was modelled as a multivariate Normal with independent components in Section 3.1. For the affordance model on the other hand, we used a different parameterization of the goal distribution that is more flexible and expressive than a Normal distribution. Specifically, we parameterized the goal distributions with categorical random variables over the discretized $[-1, 1]$ range for each dimension,

similar to how we parameterized the continuous actions.

Policy. The policy used in the LLC was the same as that used for the primitive actions in the HLC, which is that used in Muesli (Hessel et al., 2021).

B.3. High-Level Controller

For the HLC in this work, we used a Muesli agent with adaptations to the policy, so that it could select high-level actions (see Section 3.2). The primitive observations were processed as in the original Muesli agent, and the LLC observations were treated as scalar and vector observations and processed like other scalar and vector observations in Muesli—that is, input to an MLP and the result concatenated to the other processed observations. For specific hyper-parameters different from those used by Hessel et al. (2021), refer to Table 2.

Vector Goal Policy. To select vector goals in the HLC, we augmented the action space of the Muesli agent (Hessel et al., 2021) with 32 extra continuous actions, the same dimension as our continuous goal space $G \in \mathcal{G}$. We also added a Bernoulli distribution for choosing between primitive actions and options as well as additional actions for the LLC hyperparameters set by the HLC, as described in Section 3.2.

C. Additional Results

C.1. Exploring the HLC-LLC Interface and per-level performance

It was very surprising to find out that the best H2O2 performance came from the agent with maximum goal space compression, so we wanted to further investigate whether completely removing the goal space and allowing the LLC to execute an unconditional reward-maximising policy would perform at a similar level. The hypothesis is that since the goal space is strongly regularized towards a standard Normal, the *capacity* of the goal space should be quite low, and hence not much information should propagate through to

Table 1 | Training hyper-parameters for the LLC.

Network	
Image encoder (Observation)	ResNet with SAME padding
ResNet channels	(16, 32, 32)
ResNet residual blocks	(2, 2, 2)
ResNet kernel sizes	(3, 3, 3)
ResNet kernel strides	(1, 1, 1)
ResNet pool sizes	(3, 3, 3)
ResNet pool strides	(2, 2, 2)
MLP sizes	(512, 512)
Proprioceptive encoder MLP sizes	(256, 64)
State LSTM size	512
Policy conditioning	Concatenation
Policy LSTM size	512
Policy Head MLP shapes	(512, 256, 128, 196)
Number of components per continuous actions	8
Policy Distribution for continuous actions	Mixture of Clipped Logistics
Policy Distribution for discrete actions	Categorical
Value Head MLP shapes	(512, 256, 128, 1)
Number of actions	10
Goal Encoder	
Goal ResNet Encoder	Same as Observation ResNet
Goal MLP sizes	(512, 512, 256, 256, 32)
Goal activation	LayerNorm + tanh activation
Auxiliary Losses	
Behavioral Policy Head MLP	(512, 256, 128, 196)
Goal Model MLP	(512, 256, 128)
Goal Model Distribution	Binned bounded range per dim.
Number of bins per dimension	21
External State Value MLP	(256, 256, 1)
Attainment Predictor LSTM size	256
Attainment Predictor MLP sizes	(256, 256, 64)
Losses	
V-Trace discount factor γ	0.8
$\widehat{V}^{\pi_{LLC}}$ objective weight	0.5
KL-Regularizer (to Behavior Policy) weight (α in Eq. (1))	10^{-2}
Neg-entropy regularizer ($-H(\pi_{LLC})$) weight	10^{-3}
ρ clipping threshold	1
External state value discount factor	0.99
Optimizer	Adam
Learning Rate	10^{-4}
Global Norm clipping	10000
Batch size	16
Unroll Length	64
Action repeat	4

Table 2 | Training hyper-parameters for the HLC and Flat Muesli baseline. The only difference is the number of actions, where for the baseline there are only the primitive actions. For parameters we do not provide values to, refer to [Hessel et al. \(2021\)](#).

Replay proportion in batch	0.5
Discount factor	0.997
Optimizer	Adam
Learning rate	$3 \cdot 10^{-4}$
Model unroll length	2
Policy weight	3
Auxiliary weight	1
Policy Distribution for discrete actions	Categorical
Policy Distribution for continuous actions	Mixture of Clipped Logitics
Number of components per continuous action	8
Number of actions	43, factored as 1 (execute option or primitive action, binary) 32 (goal, continuous) 10 (primitive action, 8 continuous, 2 binary)
Action repeat	4

the LLC. To test this hypothesis, we implemented two variants of H2O2 with unconditional LLCs.

The first one is "Autopilot (BC)", where only the Behavioral Cloning policy, $\mu(a_t|b_t)$ (notice how the dependence of the goal g is dropped), is used for acting and trained by maximising the log-likelihood of actions. These actions come from trajectories drawn from the replay and are generated while the full agent is acting. We note that there is no special goal selection or external reward used to train the "Autopilot (BC)". This LLC variant is simply learning to re-generate experience it has already seen, and the HLC is only required to select when to deploy the LLC, rather than selecting which goals it should attend.

The second variant is "Autopilot (Vtrace)", and is trained with the same offline RL method described in Section 3.1 (Offline RL paragraph), but without the conditioning on the goal (see Eq. (1)). This means that the policy of the LLC is only conditioned on the current recurrent state, b_t , as all dependencies on a goal, g , are dropped. The data is drawn similar to "Autopilot (BC)", but now the Advantage is calculated based on the external reward. For this reason, "Autopilot (Vtrace)" is actually trained using offline data to solve the task directly, and the HLC simply

chooses when to deploy the LLC.

We compare their performance on a per-task basis with the best performing H2O2 variant used in the main report and the Flat baseline in Fig. 9. As we can see, both of these variants with unconditional, reward-maximising LLCs are performing worse than H2O2 on 3 of the tasks, and about as well on the other 3. In addition, "Autopilot (Vtrace)" performs better than the "Autopilot (BC)" on 4 out of 6 tasks, with the latter matching performance on the remaining two. This is not very surprising as the V-trace loss allows us to consume sub-optimal, off-policy data, whereas Behavioral Cloning is expected to work best when using predominantly expert data.

What is somewhat surprising though, is that there is a significant difference between the H2O2 variant with a strongly regularized goal space and an unconditional LLC. This means that even though the goal space is strongly regularized, it is still able to capture enough information and propagate it to the LLC policy. An additional final reason of the much lower performance is because none of the two Autopilot variants make use of any of the auxiliary losses mentioned in Section 3.1, which could mean that they play a significant role in shaping the LLC network.

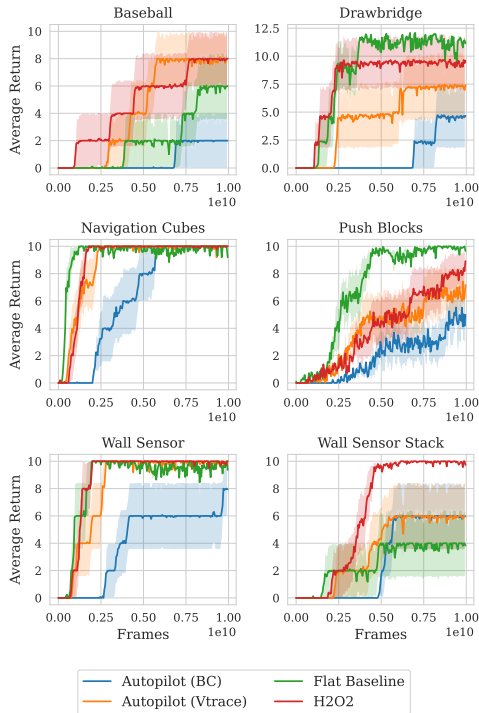


Figure 9 | Average episode return per task for different agents. We only show performance on the 6 tasks that agents made some progress, and exclude the results on Throw Across and Remember Sensor, where no agent made any progress on.

C.2. Compare the number of model parameters

We cannot attribute the increased performance solely to more parameters. Increasing the number of parameters of the flat baseline increases performance in some of the hard eight tasks, but not every way to increase parameters is effective. Even a flat baseline with more parameters fails to outperform H2O2 in one of the tasks.

We compared the performance of H2O2 against flat Muesli baselines with different number of parameters³ in Fig. 11. The H2O2 has 46M parameters (34M on the HLC, 12M on the LLC). The flat baseline presented in the paper so far has 32M parameters. We additionally experimented with a baseline with additional MLP layers (“Deeper”, 35M parameters), and a baseline with wider hidden layers (“Wider”, 68M param-

³All numbers of parameters reported are rounded to millions.

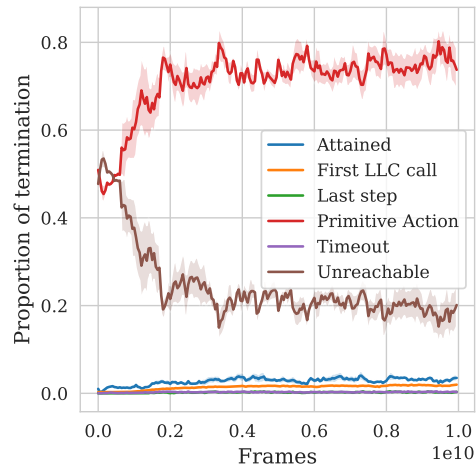


Figure 10 | Proportion of LLC execution termination reasons as training progresses.

eters) and a baseline with similar number of parameters (“Mix”, 48M parameters), achieved by both adding more layers and making the hidden layers wider. Figure 11 shows the performance of the different agents across the six tasks where performance was nontrivial, throughout training. The “Deeper” flat baseline is an example where

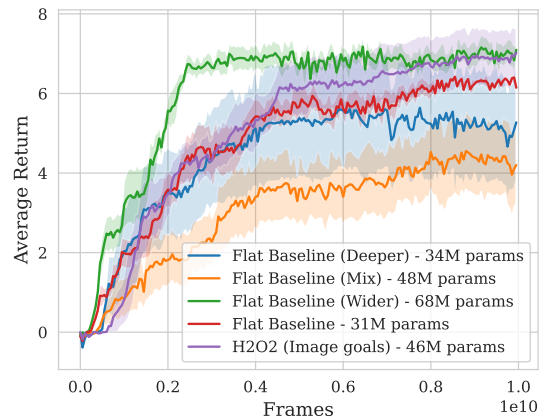


Figure 11 | Average performance of H2O2 and flat baselines with different number of parameters.

we increasing parameters but achieve worse performance. The “Wider” flat baseline has more parameters than H2O2 and matches or outperforms the flat baseline across the board. H2O2 outperforms the flat baseline in Baseball and Wall Sensor Stack. The “Wider” baseline outperforms H2O2 in Baseball, but is outperformed in Wall Sensor Stack. Surprisingly, the “Mix”

baseline performed worst than any other agent, even though it has the same number of parameters as H2O2.

We think that these results go to show that the number of parameters is not the whole story, and that carefully tuning the architecture hyperparameters, such as number of layers and their size, can have a far greater impact.

C.3. Comparing against Action Repeat

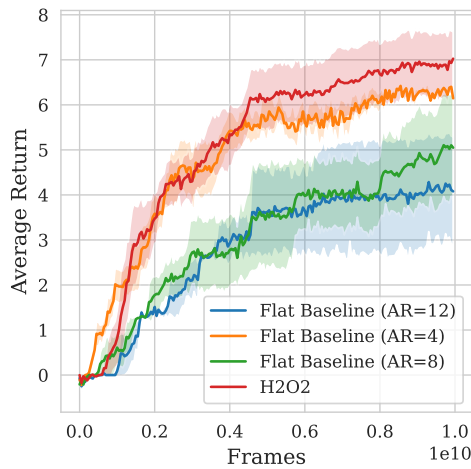


Figure 12 | The average return across levels for different action repeats (AR).

One could claim that the reason for H2O2’s strong performance is that it uses options lasting about 2 timesteps, which enable the HLC to utilize an effective action repeat of 8, rather than the actual action repeat of 4 used. To examine this claim, we have run experiments with flat baselines that instead use action repeats of 8 and 12.

As we can see in Fig. 12 though, the claim above is not supported by evidence, since the flat baselines with larger action repeats perform significantly worse. A possible reason for this is that conventional action repeats simply repeat the same action for the specified number of steps, which means that the agent loses the ability to execute different actions over that duration. This can be catastrophic for many tasks that require finer motor control, and by doing so these agent lose any benefits they might gain in terms of shorter value backups, when learning their value

function. On the contrary, since short options seem to perform at a SOTA level, it means that the primitive actions executed within the options are not simple action repeats, but most likely combinations of different primitive actions, depending on the current state of the agent.

C.4. Agent videos

We generated videos ⁴ of a trained H2O2 agent solving the different tasks from the Hard Eight suite of tasks. The video shows multiple episodes from the agent’s first-person view.

The frames in red correspond to the steps where the HLC selects an SMDP action (a primitive action or a goal), whereas the other frames refer to MDP steps where actions are selected by the LLC in response to the HLC’s SMDP action. When the LLC is executing an option per se (i.e. following a goal), the latent goal selected by the HLC is shown in the video in the “Latent Goal” box. The latent goal is a vector in $[-1, 1]^{32}$ and is visualized as a bar plot.

The “Option State Value” box shows the value estimate $\hat{V}^{x_{LLC}}$ for the given goal, over time. The rightmost point in the plot corresponds to the value estimate for the most recent timestep in the video, and the flat red line is the threshold for unattainable goals (note that points below the line are a plotting artifact as they would refer to timesteps before the option started). This plot is only valid when an option is being followed (that is, when a Latent Goal is shown).

The “Distance-to-Goal Predictor” box shows the probability estimates of the predictor for how many steps into the future the goal is attained. This plot is only valid when an option is being followed (that is, when a Latent Goal is shown).

We can see in the videos that both the Option State Value and the Distance-to-Goal Predictor probabilities behave sensibly. The option state value rises as the agent approaches the goal, and the mass over distance-to-goal shifts towards the zero bin. Once the probability mass is maximum at zero, the option terminates, as specified by the

⁴<https://youtube.com/playlist?list=PLlHafZmkZCGmIYSH09aot75l07kbiuLN0>

termination criterion.

The majority of HLC actions in the videos are primitive actions, and when goals are issued they typically last for a few steps (three to seven). The goal-following behavior we observed in the videos seem to cover navigating towards objects, picking them up and carrying them, whereas primitive actions seem to be reorienting the agent’s view.

Qualitatively, we see from the video different signs that the hierarchical behavior being learned is sound and in line with what we would expect to be useful for solving the tasks, but that specific parts of the agent’s behavior are still executed in terms of primitive actions rather than options.

C.5. Low Level Controller Heatmaps

In Fig. 13, we present a qualitative analyse of the goal-following performance of the LLC, in isolation from the HLC. The setup is the following: 100 instances of the LLC are initialized in different instances of the same evaluation `Navigation Cubes` task. Each of them is shown a goal image of a golden apple being right in front of the agent, which would have been the observation had the agent reached the golden apple. The LLCs then take actions, trying to reach the given goal. If the LLC option execution is terminated, the same goal image is presented again, for a total of 20 times per episode, for each LLC instance. We record the trajectory of every LLC instance and overlay them all on the same top-down map of the environment, where each LLC instance can be seen as a single red dot. Figure 13 shows snapshots of the overlaid trajectories at different timesteps.

At timestep 0, all instances start from the same position, and initially they move in a similar direction. After about 40 timesteps, their trajectories start to differentiate significantly, with some of them making it across the cube pit, while others end up spending a long time around the corner of the room. The main takeaway from this analysis is that indeed the different LLC instances behave similar in the beginning, but their trajectories seem to diverge at longer timescales, as they interact with the environment.

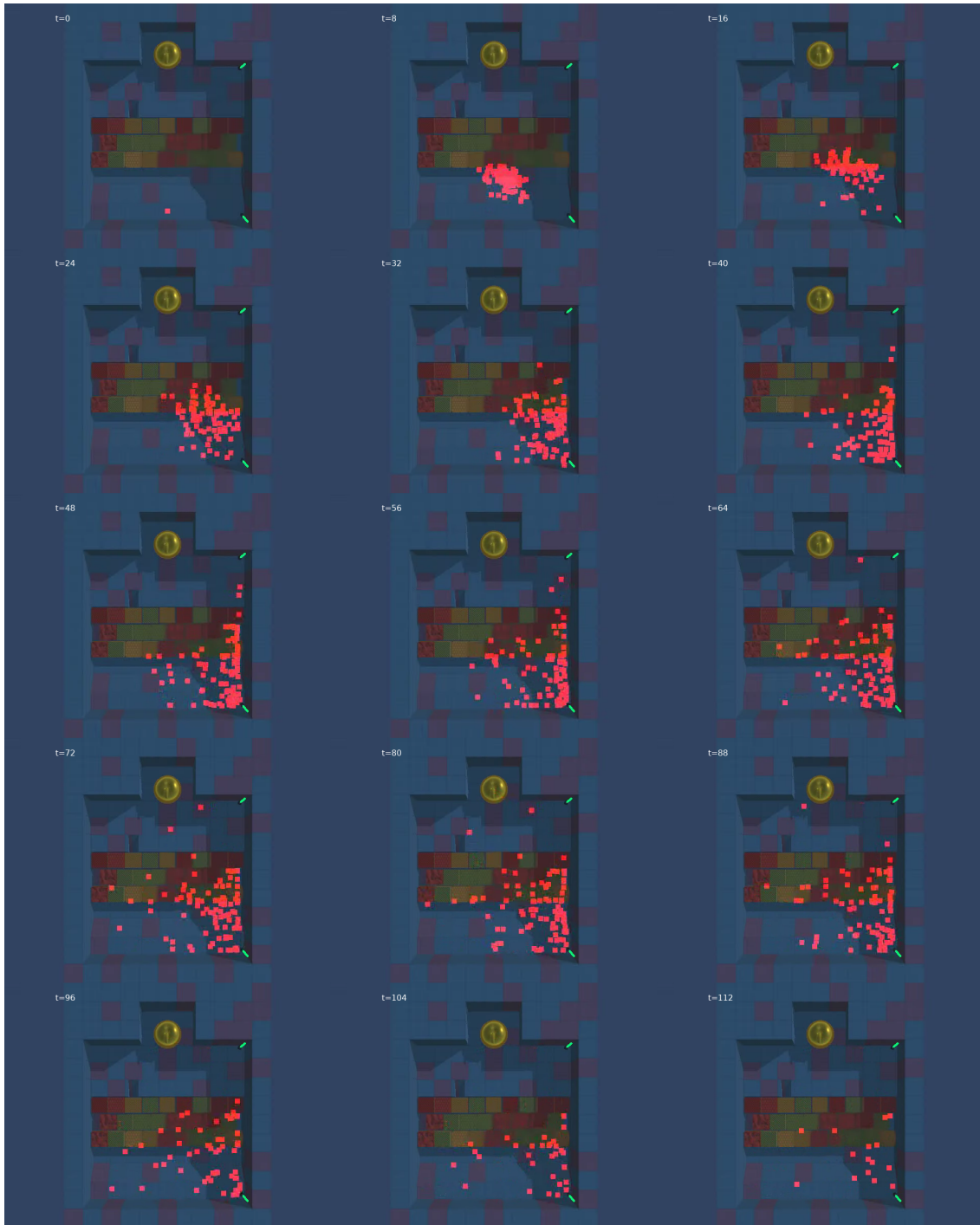


Figure 13 | Top-down positions of the LLC at different timesteps in the Navigation Cubes task. Note that there is no HLC here, as we are manually giving the same image goal of a golden apple to the LLC, for 20 repetitions. Note how all LLC instances are following a similar path towards the golden apple, with some variation. Each red dot corresponds to the position of a single LLC instance out of 100 identical LLCs initialized from the same state and given the same goal. Note that when each LLC terminates for all 20 repeated goals, or the episode terminates by reaching the apple, its corresponding red dot disappears.